AIMS Mathematics, 9(5): 12751–12777.
DOI:10.3934/math.2024623
Received: 25 January 2024
Revised: 10 March 2024
Accepted: 18 March 2024
Published: 08 April 2024

https://www.aimspress.com/journal/Math

Research article

Finite-time synchronization for fuzzy shunting inhibitory cellular neural networks

Zhangir Nuriyev[1], Alfarabi Issakhanov[1], Jürgen Kurths[2,3] and Ardak Kashkynbayev[1,*]

[1] Department of Mathematics, Nazarbayev University, Astana 010000, Kazakhstan
[2] Potsdam Institute for Climate Impact Research, Potsdam 14473, Germany
[3] Institute of Physics, Humboldt University Berlin, Berlin 10099, Germany

* **Correspondence:** Email: ardak.kashkynbayev@nu.edu.kz.

Abstract: Finite-time synchronization is a critical problem in the study of neural networks. The primary objective of this study was to construct feedback controllers for various models based on fuzzy shunting inhibitory cellular neural networks (FSICNNs) and find out the sufficient conditions for the solutions of those systems to reach synchronization in finite time. In particular, by imposing global assumptions of Lipschitz continuous and bounded activation functions, we prove the existence of finite-time synchronization for three basic FSICNN models that have not been studied before. Moreover, we suggest both controllers and Lyapunov functions that would yield a feasible convergence time between solutions that takes into account the chosen initial conditions. In general, we consecutively explore models of regular delayed FSICNNs and then consider them in the presence of either inertial or diffusion terms. Using criteria derived by means of the maximum-value approach in its different forms, we give an upper bound of the time up to which synchronization is guaranteed to occur in all three FSICNN models. These results are supported by 2D and 3D computer simulations and two respective numerical examples for 2×2 and 2×3 cases, which show the behavior of the solutions and errors under different initial conditions of FSICNNs in the presence and absence of designed controllers.

Keywords: finite-time synchronization; cellular neural networks; nonlinear partial differential equations; feedback controllers; Lyapunov function
Mathematics Subject Classification: 00A69, 34A07, 34D06, 92B20, 92C42

1. Introduction

To date, neural networks have become more important due to their high processing speeds, which help to solve complex problems in various fields. Being composed of a large number of single yet interconnected cellular units called neurons, neural networks have a lot of applications, such as image

and signal processing, combinatorial optimization, associative memories, fault diagnosis, ocean remote sensing, and pattern recognition. Therefore they can be specifically defined from the prism of the subject of interest. We, however, will focus on their role in the construction of principles based on which the human brain operates. For that purpose, we will also be required to introduce time-varying delay to the neural networks because of the additional dynamical behaviors its presence grants the model [1]. It would particularly help to improve the modeled system's approximated accuracy because it takes into account the strong connection of neurons, which is not surprising as the state of the preceding unit should affect the state of the following one. To make one's model more suited to characterize the actual processes occurring between neurons, one should add one or more hidden layers that comprise shunting neurons so that their linear combination would enable control of the output values of the produced inhibition [2]. Consequently, the basic synaptic interaction of hidden units is often used to build cellular neural networks (CNNs) as it has been proven to be an effective tool in robotics as well as in different vision problems. For example, it helps to enhance edges, visual selectivity of small objects, and contrast [3]. The introduction of fuzzy terms and time-varying delays is essential for challenging problems because of their effects on the ability to mimic human thinking and perception [4].

The importance of the synchronization concept has been recognized already by Huygens [5]. However, there has been increasing interest recently due to its role in complex systems and its versatile applications in cryptography, pseudo random number generators, secure communication, power convertors, and information processing [6]. While dealing with such problems, the goal of increasing importance is to create a synchronization procedure which converges in either finite or fixed time. It is also well-known that in the resultant master-slave configuration the slave state is expected to constantly follow the master's trajectory. The development of special controllers and different Lyapunov functionals allows for the development of sufficient conditions to observe synchronization at some point in time. Finite-time synchronization is considered to be practical as it would be feasible to calculate the maximum convergence time in advance unlike the rest of the synchronization classes that can typically only be realized as time tends to infinity. This is the major reason why many studies have focused on this problem. Moreover, since the primary requirement is to have a finite settling time, several helpful lemmas and techniques that encompass robustness and disturbance rejection properties shall be used in this paper [7]. Liu et al. [8] explained the importance of finite-time synchronization by stating that the solutions must realize it, as one would consequently possess the precise data needed for the successful completion of a lot of tasks. This characteristic is fundamental to the comprehension of more complex systems.

In this study, we intended to work with the aforementioned constructs by using the maximum principle. This substantial tool gained its popularity for allowing the user to obtain crucial pieces of information about solutions to differential equations and inequalities in the absence of the demand to explicitly derive them. Consequently, physicists, chemists, engineers, and economists have found suitable applications of this method thanks to its ability to be adapted to suit manifold problems [9]. Such a procedure was utilized in a series of modern papers in various forms [10, 11]. As for our problem, the described tool is preferred because it allows us to examine the model on a deeper level as well as to receive approximate solutions to nonlinear networks. Furthermore, since we are treating the equation as a biological pattern, we are solely interested in its positive solutions and in this setup, the maximum principle approach can be used most efficiently.

It should be emphasized that so far only well-posedness types of the introduced model have been studied [12]. However, this neither covers the controller design for the finite-time synchronization of its solutions nor includes time-dependent delays. Still, recently, many researchers have been attracted to the issue of control of networks. Considering neural networks as a whole, some scholars [13, 14] analyzed the synchronization of simpler neural networks by applying varying techniques to construct Lyapunov functions and perform its subsequent analysis to prove the solutions' convergence. Alternatively, studies have been concentrating solely on the synchronization of discrete-time fuzzy networks [15], memristive inertial networks [16], or the ones containing stochastic perturbations [17]. There have also been investigations of prescribed-time synchronization in networks of piecewise smooth systems that employ the linear matrix inequality based on a feedback control scheme as well as in the presence of impulse effects [18, 19]. Furthermore, pinning control of the robust synchronization of a class of nonlinearly coupled complex networks has been addressed by using the adaptive method as well [20]. It is worth mentioning that some recent papers focused on Hopf bifurcation analysis for chaotic CNNs [21] and adaptive finite-time synchronization of fractional-order delayed fuzzy CNNs [22]. Despite that, to the best of our knowledge, no one has considered neural networks with delays, shunting inhibition processes among neurons, and function fuzziness in the presence of either inertial or diffusion terms at the same time. The approaches to such problems include, for example, pinning control strategies for pinned nodes of nonlinear complex networked systems that rely on more traditional lemmas [23, 24]. On the other hand, specifically designed controllers that will be suitable for employing the maximum principle and chosen Lyapunov functions are presented in this paper. Such a combination will demonstrate the convenient and computationally favorable way of proving the occurrence of synchronization between solutions of the model that involves various parameters and phenomena in finite time. This is the main reason why we intend to analyze these described network configurations. As a result, we chose to employ techniques based on the maximum principle and several relevant inequalities. This work provides different controllers for the given models under realizable preliminary assumptions that lead to synchronization in finite time. Furthermore, the obtained theoretical results are supported by illustrative examples and numerical simulations.

By pointing out the correlation between different processes in time, synchronization itself is regarded as one of the most complicated but also efficient dynamics present in CNNs, as compared to the well-studied stability analysis or periodic oscillations. The advanced model we investigate is very close to a real system, as it resembles an electric circuit with synaptic activity that transmits a signal across a large set of cells. Moreover, it should be noted that to include any oscillation phenomena or network instability that can occur in such circuit representations due to the finite switching speed of amplifiers and the inherent communication time of neurons, interactive time delays have been added to the model equation [25]. As a consequence, the system that is currently under consideration includes delays that would improve otherwise robust interactions between nodes in the presence of a strange attractor. It also features an effective and easily implementable feedback controller that allows us to use versatile approaches of the classical maximum principle. The main idea of this powerful yet easily adaptable method is that functions that satisfy the condition of a differential inequality in a domain D achieve their maxima at its boundary [26]. To the best of our knowledge, nobody has used this to prove solution convergence in more complex networks, especially in the presence of fuzziness. These challenges are included in the basic problem, given in matrix form as follows:

$$\frac{dx(t)}{dt} = -Dx(t) + Ag(x(t)) + Bf(x(t-\tau)) + I(t),$$

where $x(t) = [x_1(t), ..., x_n(t)]^T, D = diag\{d_1, ..., d_n\}, d_k > 0, A = (a_{kl}), B = (b_{kl})$, $k, l = 1, 2, ..., n, g(x) = [g_1(x_1), ..., g_n(x_n)]^T, f(x(t-\tau)) = [f_1(x_1(t-\tau)), ..., f_n(x_n(t-\tau))]^T$ and $I(t) = [I_1(t), ..., I_n(t)]^T$. It is then extended by adding an amplification gain as below.

$$\dot{x}_i(t) = -d_i\left(c_i(x_i(t)) - \sum_{j=1}^{n} a_{ij}f_j x_j(t) + \sum_{j=1}^{n} b_{ij}f_j(x_j(t-\tau)) + J_i\right), i = 1, ..., n$$

Others proceeded with an even more comprehensive formulation involving a coupling delay, as shown below.

$$\begin{aligned}\frac{dx_i(t)}{dt} =& - Cx_i(t) + Af(x_i(t)) + Bf(x_i(t-\tau)) + I(t) + \sum_{j=1}^{N} G_{ij}Dx_j(t) \\ &+ \sum_{j=1}^{N} G_{ij}D_\tau x_j(t-\tau), i = 1, 2, ..., N\end{aligned}$$

We, on the other hand, further extend the formulation by adding fuzzy operations to represent the transmission between cells and differentiate between external input and external force applied to a particular cell.

Motivated by the above discussion, we organized our paper to comprise three parts. We will start by analyzing the synchronization of the solutions to the regular FSICNNs and proceed by consecutively adding the inertial and diffusion terms to the existing model. Finally, numerical examples together with simulations confirming the proofs will be provided as well.

2. Synchronization of the FSICNN

By taking into account the phenomenon of fuzziness and fuzzy logic theory, one would have the mathematical strength to handle uncertainties occurring in neural networks. This was manifested in the introduction of fuzzy CNNs (FCNNs), which can be regarded as a representation of CNNs from the perspective of fuzzy operator usage in the synaptic computation [27]. Furthermore, the design of FCNNs that preserves both local connectedness between neurons and simple cell structures is of great importance in the image-processing paradigm, including in edge detection and medial axis transformation [28]. Moreover, cognitive science has proven to be a field in which FCNNs can be extensively applied because human cognitive processes and neural systems involve a lot of ambiguities. As a result, modern scientists have become very interested in studying the dynamics of FCNNs. To be more precise, their scientific value lies in the ability to simulate typical human reasoning ability in a computationally efficient way [29]. That is the primary reason why we would like to analyze the synchronization of regular delayed shunting inhibitory cellular neural networks in the presence of fuzziness, which are widely spread among medical diagnosis problems [30]. As for the emergence of the concept of a fuzzy neuron, as inspired by the McCulloch-Pitts model, it improves the adaptability better the systems' overall behavior as they can often be defined imprecisely because of their high

degree of complexity [31]. Therefore, the incredible flexibility and adaptability of biological neuronal control mechanisms that are provided by the fuzzy terms in the system equation are considered to be a convincing source of motivation and framework for the design of intelligent and autonomous robots [32].

The presented first-order linear differential equation will describe the change of the voltage input to the cells inside the neural network, which can be represented as an electrical circuit. The mathematical model can be derived by using techniques from electrical engineering, such as Kirchhoff's current and voltage laws. We begin with the consideration of the network in the following form:

$$\begin{aligned}\dot{x}_{ij}(t) =& - a_{ij}(t)x_{ij}(t) - \sum_{C_{kl}\in N_r(i,j)} C_{ij}^{kl}(t)f_{ij}(x_{kl}(t))x_{ij}(t) + L_{ij}(t) + \sum_{C_{kl}\in N_r(i,j)} B_{ij}^{kl}(t)U_{ij}(t)\\ &- \bigwedge_{C_{kl}\in N_r(i,j)} D_{ij}^{kl}(t)f_{ij}(x_{kl}(t-\tau_{kl}(t)))x_{ij}(t) - \bigvee_{C_{kl}\in N_r(i,j)} E_{ij}^{kl}(t)f_{ij}(x_{kl}(t-\tau_{kl}(t)))\\ &\times x_{ij}(t) + \bigwedge_{C_{kl}\in N_r(i,j)} T_{ij}^{kl}(t)U_{ij}(t) + \bigvee_{C_{kl}\in N_r(i,j)} H_{ij}^{kl}(t)U_{ij}(t), \end{aligned} \tag{2.1}$$

where C_{ij}, $i = 1, 2, \ldots, z$, $j = 1, 2, \ldots, n$, denotes the cell at the (i, j) position of the lattice; the $r-$neighborhood of C_{ij} is $N_r(i, j) = \{C_{kl} : \max\{|k - i|, |l - j|\} \leq r,\ 1 \leq k \leq z,\ 1 \leq l \leq n\}$; x_{ij} represents the activity of the cell C_{ij} at time t; the positive functions denoted by $a_{ij}(t)$ represent the passive decay rate of the cell activity; $U_{ij}(t)$ denotes the external input, whereas $L_{ij}(t)$ reflects the external force applied on the (i, j)th cell; the non-negative functions $C_{ij}^{kl}(t)$, $D_{ij}^{kl}(t)$, $E_{ij}^{kl}(t)$, $T_{ij}^{kl}(t)$, and $H_{ij}^{kl}(t)$ represent the connection or coupling strength of the postsynaptic activity, the fuzzy feedback MIN template, fuzzy feedback MAX template, fuzzy feed forward MIN template, and fuzzy feed forward MAX template of the cell C_{kl} transmitted to the cell C_{ij} at time t, respectively; $\bigwedge$ is the fuzzy AND operation whereas $\bigvee$ is the fuzzy OR operation; the functions denoted by $f(x_{kl})$ represent the measures of activation to the output or firing rate of the cell C_{kl}; and τ_{kl} corresponds to the transmission delay along the axon of the (k, l)th cell from the (i, j)th cell, $\Gamma_1 = \{1, 2, \ldots, z\}$ and $\Gamma_2 = \{1, 2, \ldots, n\}$.

In addition to that, it will be required to include the following generalized assumptions listed below.

(A1) The function $f(\cdot) = [f_{11}(\cdot), \ldots, f_{zn}(\cdot)]$ is Lipschitz continuous on $\mathbb{R}$ with the Lipschitz constant L^f i.e., $|f(x) - f(y)| \leq L^f|x - y|$;

(A2) There exists a constant M such that $|f(x)| \leq M$;

(A3) Introducing the parameters

$$\begin{aligned}\sigma =& \max_{(i,j)}\{|x_{ij}(0)|\}, \upsilon = \sup\left(L_{ij}(t) + U_{ij}(t)\sum_{C_{kl}\in N_r(i,j)}\left(B_{ij}^{kl}(t) + T_{ij}^{kl}(t) + H_{ij}^{kl}(t)\right)\right),\\ \kappa =& \sigma\left(1 - M\sup\sum_{C_{kl}\in N_r(i,j)}\left(C_{ij}^{kl}(t) + D_{ij}^{kl}(t) + E_{ij}^{kl}(t)\right)\right),\end{aligned}$$

the inequality $\upsilon < \kappa$ must hold.

The next lemma will also be of significant importance throughout the whole analysis.

Lemma 1 ([33]). *If both $x, y \in \mathbb{R}$ solve the network* (2.1)*, then the following pair of inequalities is valid:*

$$\left|\bigwedge_{C_{kl}\in N_r(i,j)} D_{ij}^{kl}(t)f_{ij}(x) - \bigwedge_{C_{kl}\in N_r(i,j)} D_{ij}^{kl}(t)f_{ij}(y)\right| \leq \sum_{C_{kl}\in N_r(i,j)}\left|D_{ij}^{kl}(t)\right|\left|f_{ij}(x) - f_{ij}(y)\right|,$$

$$\Big|\bigvee_{C_{kl}\in N_r(i,j)} E_{ij}^{kl}(t)f_{ij}(x) - \bigvee_{C_{kl}\in N_r(i,j)} E_{ij}^{kl}(t)f_{ij}(y)\Big| \le \sum_{C_{kl}\in N_r(i,j)} \big|E_{ij}^{kl}(t)\big|\big|f_{ij}(x) - f_{ij}(y)\big|.$$

For convenience, one can rewrite (2.1) in the following form:

$$\dot{x}_{ij}(t) = -a_{ij}(t)x_{ij}(t) + R_{ij}(x(t),t), \tag{2.2}$$

where

$$\begin{aligned} R_{ij}(x(t),t) =& L_{ij}(t) + \sum_{C_{kl}\in N_r(i,j)} B_{ij}^{kl}(t)U_{ij}(t) - \bigwedge_{C_{kl}\in N_r(i,j)} D_{ij}^{kl}(t)f_{ij}(x_{kl}(t-\tau_{kl}(t)))x_{ij}(t) \\ &- \bigvee_{C_{kl}\in N_r(i,j)} E_{ij}^{kl}(t)f_{ij}(x_{kl}(t-\tau_{kl}(t)))x_{ij}(t) + \bigwedge_{C_{kl}\in N_r(i,j)} T_{ij}^{kl}(t)U_{ij}(t) \\ &+ \bigvee_{C_{kl}\in N_r(i,j)} H_{ij}^{kl}(t)U_{ij}(t) - \sum_{C_{kl}\in N_r(i,j)} C_{ij}^{kl}(t)f_{ij}(x_{kl}(t))x_{ij}(t). \end{aligned}$$

The response is consequently denoted by

$$\dot{y}_{ij}(t) = -a_{ij}(t)y_{ij}(t) + R_{ij}(y(t),t) + p_{ij}(t) \tag{2.3}$$

and the error system is just the difference, i.e.,

$$\dot{e}_{ij}(t) = -a_{ij}(t)e_{ij}(t) + \Delta R_{ij}(x(t),y(t)) + p_{ij}(t)$$

provided that

$$\begin{aligned} \Delta R_{ij}(x(t),y(t)) =& -\sum_{C_{kl}\in N_r(i,j)} C_{ij}^{kl}(t)\Big(f_{ij}(y_{kl}(t))y_{ij}(t) - f_{ij}(x_{kl}(t))x_{ij}(t)\Big) \\ &- \bigwedge_{C_{kl}\in N_r(i,j)} D_{ij}^{kl}(t)\Big(f_{ij}(y_{kl}(t-\tau_{kl}(t)))y_{ij}(t) \\ &- f_{ij}(x_{kl}(t-\tau_{kl}(t)))x_{ij}(t)\Big) - \bigvee_{C_{kl}\in N_r(i,j)} E_{ij}^{kl}(t) \\ &\times \Big(f_{ij}(y_{kl}(t-\tau_{kl}(t)))y_{ij}(t) - f_{ij}(x_{kl}(t-\tau_{kl}(t)))x_{ij}(t)\Big). \end{aligned}$$

The proof of the lemma below is identical to the one from the source paper and will be omitted.

Lemma 2 ([34]). *Supposing that (A1)–(A3) are valid, if* $|x_{ij}(0)| \le \sigma$, *it follows that* $|x_{ij}(t)| \le \sigma$ *whenever* $t \ge 0, 1 \le i \le z$ *and* $1 \le j \le n$.

Recalling that, according to the definition, our goal is to show that there exists $T > 0$ such that $\lim_{t\to T}|y_{ij}(t) - x_{ij}(t)| = 0$ and $|y_{ij}(t) - x_{ij}(t)| = 0, \forall t > T$, and denoting $\inf a_{ij}(t) = \underline{a}$, $\sup \sum_{(i,j)} |C_{ij}^{kl}(t)| = \bar{C}$, $\sup \sum_{(i,j)} |D_{ij}^{kl}(t)| = \bar{D}$, $\sup \sum_{(i,j)} |E_{ij}^{kl}(t)| = \bar{E}$, the theorem below can be formulated.

Theorem 1. *Assuming that* $\underline{a} > 1+\left(\bar{C}+\bar{D}+\bar{E}\right)\left(M+L^f\sigma\right)$, *for the Lyapunov function* $M(t)=\sum_{(i,j)} e_{ij}^2(t)$ *and controller* $p_{ij}(t)=\begin{cases}\frac{e_{ij}^2(t)-e_{ij}(t)+\frac{g}{2\sqrt{t+m}}-\frac{d+H}{2}}{e_{ij}(t)} & \text{if } g,m,H>0, d>\frac{1}{2\left(\underline{a}-1-\left(\bar{C}+\bar{D}+\bar{E}\right)\left(M+L^f\sigma\right)\right)}\\ 0, & \text{whenever } e_{ij}(t)=0\end{cases}$, (2.2) *and* (2.3) *achieve finite-time synchronization at* $t_0=\frac{2g^2+M(0)H+2g\sqrt{g^2+(M(0)+mH)H}}{H^2}$.

Proof. First, we can express the following:

$$\begin{aligned}
|\Delta R_{ij}(x,u)| &= \sum_{C_{kl}\in N_r(i,j)} C_{ij}^{kl}(t)\Big(f_{ij}(x_{kl}(t))x_{ij}(t)-f_{ij}(u_{kl}(t))u_{ij}(t)\Big)\\
&\quad+\left(\bigvee_{C_{kl}\in N_r(i,j)} E_{ij}^{kl}(t)+\bigwedge_{C_{kl}\in N_r(i,j)} D_{ij}^{kl}(t)\right)\Big(f_{ij}(x_{kl}(t-\tau_{kl}(t)))x_{ij}(t)\\
&\quad-f_{ij}(u_{kl}(t-\tau_{kl}(t)))u_{ij}(t)\Big)\\
&\le \sum_{C_{kl}\in N_r(i,j)} C_{ij}^{kl}(t)\Bigg[f_{ij}(x_{kl}(t))x_{ij}(t)-\left(\bigvee_{C_{kl}\in N_r(i,j)} E_{ij}^{kl}(t)+\bigwedge_{C_{kl}\in N_r(i,j)} D_{ij}^{kl}(t)\right)\\
&\quad\times f_{ij}(u_{kl}(t))x_{ij}(t)+f_{ij}(u_{kl}(t))x_{ij}(t)-f_{ij}(u_{kl}(t))u_{ij}(t)\Bigg]\\
&\quad+\left(\sum_{C_{kl}\in N_r(i,j)} E_{ij}^{kl}(t)+\sum_{C_{kl}\in N_r(i,j)} D_{ij}^{kl}(t)\right)\Big(f_{ij}(x_{kl}(t-\tau_{kl}(t)))x_{ij}(t)\\
&\quad-f_{ij}(u_{kl}(t-\tau_{kl}(t)))x_{ij}(t)+f_{ij}(u_{kl}(t-\tau_{kl}(t)))x_{ij}(t)\\
&\quad-f_{ij}(u_{kl}(t-\tau_{kl}(t)))u_{ij}(t)\Big)\\
&\le\Big(\sum_{C_{kl}\in N_r(i,j)} C_{ij}^{kl}(t)+\sum_{C_{kl}\in N_r(i,j)} E_{ij}^{kl}(t)+\sum_{C_{kl}\in N_r(i,j)} D_{ij}^{kl}(t)\Big)\\
&\quad\times\left(L^f|x_{ij}(t)|+M\right)|x_{ij}(t)-u_{ij}(t)|. \qquad (2.4)
\end{aligned}$$

One can also observe the following:

$$\begin{aligned}
M'(t) &\le 2\sum_{(i,j)} e_{ij}(t)[-a_{ij}(t)e_{ij}(t)+\Delta R_{ij}(x(t),y(t))+p_{ij}(t)]\\
&\le 2\sum_{(i,j)}\Big(-a_{ij}(t)e_{ij}^2(t)+\left(\bar{C}+\bar{D}+\bar{E}\right)(M+L^f|x|)e_{ij}^2(t)+p_{ij}(t)e_{ij}(t)\Big)\\
&\le \sum_{(i,j)}\Big(2e_{ij}^2(t)\left(1-\underline{a}+\left(\bar{C}+\bar{D}+\bar{E}\right)\left(M+L^f\sigma\right)\right)-2e_{ij}(t)-d-H+\frac{g}{\sqrt{t+m}}\Big).
\end{aligned}$$

Now we need to introduce the equation

$$G(e)=2e_{ij}^2(t)\left(1-\underline{a}+\left(\bar{C}+\bar{D}+\bar{E}\right)\left(M+L^f\sigma\right)\right)-2e_{ij}(t)-d$$

so that its critical point is located at

$$e_0 = \frac{1}{2\left(1 - \underline{a} + \left(\bar{C} + \bar{D} + \bar{E}\right)(M + L^f\sigma)\right)}.$$

Besides, the substitution of

$$J = \left(\bar{C} + \bar{D} + \bar{E}\right)\left(M + L^f\sigma\right)$$

would, in turn, yield

$$\frac{d^2G}{de_{ij}^2} = 4\left(1 - \underline{a} + J\right) < 0,$$

suggesting that the extreme point is a maximum. As a consequence,

$$G(e_0) = \frac{1}{2\left(\underline{a} - 1 - J\right)} - d < 0.$$

This is used to claim that this function does not exceed the value of zero, i.e.,

$$G(e_{ij}(t)) \leq \max_{e(t)\in\mathbb{R}} G(e(t)) \leq 0.$$

So we are left with

$$M'(t) \leq \frac{g}{\sqrt{t+m}} - H.$$

By integrating both sides of the obtained inequality, we find that

$$0 \leq M(t) \leq M(0) - Ht + 2g\sqrt{t+m} \leq 0 \text{ at } t = t_0$$

which can be calculated by solving the following equation:

$$H^2t^2 + M^2(0) - 2HtM(0) = 4g^2(t+m).$$

Therefore,

$$\lim_{t\to t_0} M(t) = \lim_{t\to t_0} |e_{ij}(t)| = 0, t \in (t_0, +\infty).$$

3. Synchronization of inertial FSICNN

Inertial manifolds are widely known for being positively invariant Lipschitz spaces and having a global attractor inside them so that they can become exponentially stable in the presence of exterior perturbations [35]. For these properties, the inclusion of the corresponding term in the equation is common in nonlinear dissipative evolutionary partial differential equations(PDEs), which are often a primary choice to model actual physical systems and allow us to understand their dynamics in both

finite- and infinite-dimensional spaces [36]. For instance, phase transitions, convection, reaction-diffusion equations, and hydrodynamic instability problems were in fact based on inertial forms [37]. The advantageous aspect is the existence of numerous techniques that show that the whole system's analysis can be reduced to the study of the dynamics of ordinary differential equations. It is also essential to understand the significance of inertia in studies of neural networks, especially the fact that such a term's presence provides the foundation for the further inclusion of both chaotic phenomena and bifurcation behavior due to its inductive properties [38], which cannot be found in first-order systems [39]. One of the first acknowledged models is given by

$$x_i''(t) = -a_i(t)x_i'(t) - b_i(t)x_i(t) + \sum_{j=1}^{n} c_{ij}F_j(x_j(t)) + \sum_{j=1}^{n} d_{ij}D_j(x_j(t-\tau_j)) + J_i(t),$$
$$i \in \{1, 2, ..., n\}.$$

which, as it can clearly be seen, unlike the purely first order derivative states of neurons, includes the influence of inductors in the artificial model. By adding inertial terms in electronic neural networks, we have better control over possible complicated behaviors, whether it is instability or spontaneous oscillation about fixed points [40]. As a result, consideration of inertial networks facilitates a clearer reflection of the characteristics of biological systems and automated control [41]. We now begin by defining explicitly an inertial FSICNN:

$$\frac{d^2x_{ij}(t)}{dt^2} = -b_{ij}(t)x_{ij}'(t) - a_{ij}(t)x_{ij}(t) + R_{ij}(x(t)). \tag{3.1}$$

It can be represented as a system of first-order linear equations:

$$y_{ij}(t) = x_{ij}'(t) + x_{ij}(t) \implies x_{ij}'(t) = y_{ij}(t) - x_{ij}(t).$$
$$y_{ij}'(t) = x_{ij}''(t) + x_{ij}'(t) = y_{ij}(t) - x_{ij}(t) + R(x_{ij}(t)) - a_{ij}(t)x_{ij}(t) - b_{ij}(t)\left(y_{ij}(t) - x_{ij}(t)\right).$$

Adding the respective controllers, one gets the following system:

$$\begin{cases} x_{ij}'(t) = y_{ij}(t) - x_{ij}(t) + p_{ij}(t) \\ y_{ij}'(t) = x_{ij}(t)(b_{ij}(t) - a_{ij}(t) - 1) + y_{ij}(t)(1 - b_{ij}(t)) + R(x_{ij}(t)) + q_{ij}(t), \end{cases} \tag{3.2}$$

while the drive system of (3.2) is then

$$\begin{cases} u_{ij}'(t) = v_{ij}(t) - u_{ij}(t) \\ v_{ij}'(t) = u_{ij}(t)(b_{ij}(t) - a_{ij}(t) - 1) + v_{ij}(t)(1 - b_{ij}(t)) + R(u_{ij}(t)). \end{cases} \tag{3.3}$$

Thus, the error system is represented as

$$\begin{cases} e_{ij}'(t) = r_{ij}(t) - e_{ij}(t) + p_{ij}(t) \\ r_{ij}'(t) = e_{ij}(t)(b_{ij}(t) - a_{ij}(t) - 1) + r_{ij}(t)(1 - b_{ij}(t)) + \Delta R_{ij}(x, u) + q_{ij}(t). \end{cases} \tag{3.4}$$

We first need an additional lemma that can be stated in the following way:

Lemma 3 ([42]). *If $A > e^{-1}, x > 0$, then $-Ax + \ln x \leq 0$.*

Remark 1. *It is straightforward enough to prove that* $-Ax + \ln(\ln x) \leq 0$*, which is considered to be a corollary to the above lemma.*

Theorem 2. *Given the controllers* $p_{ij}(t) = \operatorname{sgn}\left(e_{ij}(t)\right)\left(|e_{ij}(t)| + \ln|e_{ij}(t)|\right)$ *and* $q_{ij}(t) = \operatorname{sgn}\left(r_{ij}(t)\right)\left(|r_{ij}(t)| - \ln(t+s) - l + \ln\left(\ln|r_{ij}(t)|\right)\right)$, $s, l > 0$*, then* (3.3) *and* (3.2) *achieve finite-time synchronization at* $t_1 = \max\left\{\frac{\sum_{(i,j)}(|e_{ij}(0)| + |r_{ij}(0)|)}{l}, e - s\right\}$ *if* $b_{ij}(t) \in \left(3 + \frac{1}{e}, \underline{a} - J + \frac{e-1}{e}\right)$.

Proof. Let $K(t) = \sum_{(i,j)}(|e_{ij}(t)| + |r_{ij}(t)|)$, so its differentiation yields

$$\begin{aligned}
K'(t) = \sum_{(i,j)} \Big\{ & \operatorname{sgn}(e_{ij}(t))\left(-e_{ij}(t) + r_{ij}(t) + p_{ij}(t)\right) + \operatorname{sgn}(r_{ij}(t) \\
& \times \left(-(b_{ij}(t) - 1)r_{ij}(t) + e_{ij}(t)\left(b_{ij}(t) - a_{ij}(t) - 1\right) + \Delta R_{ij}(x,u) + q_{ij}(t)\right) \Big\} \\
\leq \sum_{(i,j)} \Big\{ & r_{ij}(t)\operatorname{sgn}(e_{ij}(t)) + \ln|e_{ij}(t)| - |r_{ij}(t)|(b_{ij}(t) - 1) + \left|\Delta R_{ij}(x,u)\right| \\
& + |e_{ij}(t)|(b_{ij}(t) - a_{ij}(t) - 1) + |r_{ij}(t)| + \ln(\ln(|r_{ij}(t)|)) - \ln(t+s) - l \Big\} \\
\leq \sum_{(i,j)} \Big\{ & -|e_{ij}(t)|\left(a_{ij}(t) + 1 - b_{ij}(t)\right) - J + \ln|e_{ij}(t)| - (b_{ij}(t) - 3)|r_{ij}(t)| \\
& + \ln(\ln(|r_{ij}(t)|)) - \ln(t+s) - l \Big\}
\end{aligned}$$

This means that $K'(t) \leq -l - \ln(t+s)$ and $0 \leq K(t) \leq K(0) + t(1-l) - t\ln(t+s)$; thus, one can conclude that $\lim_{t\to t_1} K(t) = \lim_{t\to t_1}|e_{ij}(t)| = \lim_{t\to t_1}|r_{ij}(t)| = 0$.

4. Synchronization of the FSICNN with diffusion

As for the last case, it is necessary to take into account a diffusion term too, because it describes the interaction between cells at a completely new level. To be more precise, whenever an electron moves in a nonuniform electromagnetic field, in order to see a full picture of the dynamic features of a network consisting of multiple layers, thereby visualizing it in 3 dimensions, the evolution time and spatial position of the node state should be considered [43]. This statement can be supported by noting that the diffusion phenomenon must always be taken into account whenever electrons enter asymmetric electromagnetic fields. This is considered to be the main motivation to start taking a closer look at reaction-diffusion systems [44]. We can encounter its manifestations in many natural fields, particularly in chemistry, biology, and engineering, as it is an integral part of the reactions between elements [45]. Lastly, our model should contain this term because whether it is an artificial or biological neural network, consideration of the variation of states in both space and time is vital in the design of more complex systems like firing processes in brain neurons and fibrillation [46]. This paper will address the controlling issue by proposing a feedback controller that would be suitable for

PDEs based on an FSICNN. This challenge should be overcome to make full use of the advantages of introducing the diffusion term following an improvement of the approximation for a neural network in theory and applications. As a consequence, if left neglected, it may lead to such unwanted or even harmful processes as bifurcation, oscillation, divergence, or instability [47]. One of the most studied models that describe the neural dynamics' spatiotemporal properties is presented as follows:

$$\frac{\partial z_{ij}(t,x)}{\partial t} = d_j \Delta z_{ij}(x,t) - \sum_{k=1}^{M} a_{jk} z_{ik}(x,t) + \sum_{k=1}^{M} b_{jk} f_k(z_{ik}(x,t)).$$

Since there are insufficient studies focusing on proving synchronization in finite time of a neural network that feature diffusion and fuzzy terms using the computationally fast maximum-value approach, we are now going to study a more general problem. Here we are dealing with the modified nonlinear system of PDEs:

$$\frac{\partial \chi_{ij}(t,x)}{\partial t} = b_{ij}(t)\frac{\partial^2 \chi_{ij}(t,x)}{\partial x^2} - Z_{ij}(\chi(t,x),t)\chi_{ij}(t,x) + F_{ij}(t), \tag{4.1}$$

provided that

$$\begin{aligned} Z_{ij}(x(t),t) = a_{ij}(t) &+ \bigwedge_{C_{kl}\in N_r(i,j)} D_{ij}^{kl}(t) f_{ij}(\chi_{kl}(x,t-\tau_{kl}(t))) \\ &+ \bigvee_{C_{kl}\in N_r(i,j)} E_{ij}^{kl}(t) f_{ij}(\chi_{kl}(x,t-\tau_{kl}(t))) + \sum_{C_{kl}\in N_r(i,j)} C_{ij}^{kl}(t) f_{ij}(\chi_{kl}(t,x)), \\ F_{ij}(t) = L_{ij}(t) &+ \sum_{C_{kl}\in N_r(i,j)} B_{ij}^{kl}(t) U_{ij}(t) + \bigwedge_{C_{kl}\in N_r(i,j)} T_{ij}^{kl}(t) U_{ij}(t) \\ &+ \bigvee_{C_{kl}\in N_r(i,j)} H_{ij}^{kl}(t) U_{ij}(t). \end{aligned}$$

On the other hand, the slave system is as follows:

$$\frac{\partial y_{ij}(t,x)}{\partial t} = b_{ij}(t)\frac{\partial^2 y_{ij}(t,x)}{\partial x^2} - Z_{ij}(y(t,x),t)y_{ij}(t,x) + F_{ij}(t) + r_{ij}(x,t) \tag{4.2}$$

The error equation is then

$$\begin{aligned} \frac{\partial e_{ij}(t,x)}{\partial t} =& b_{ij}(t)\frac{\partial^2 e_{ij}(t,x)}{\partial x^2} - \Big(Z_{ij}(y(t,x),t)y_{ij}(t,x) - Z_{ij}(\chi(t,x),t)\chi_{ij}(t,x)\Big) \\ &+ r_{ij}(x,t). \end{aligned} \tag{4.3}$$

Initial and boundary conditions will take the following form:

$$\begin{aligned} e_{ij}(t,x) =& 0, (t,x) \in [-\tau,+\infty)\times\partial\Omega, \\ e_{ij}(s,x) =& \phi_{ij}(s,x) - \mu_{ij}(s,x), (s,x) \in [-\tau,0]\times\Omega, \text{ where } \Omega = \{h^g \le x \le h^G\} \subset \mathbb{R}^m. \end{aligned}$$

Additionally, the following three lemmas will be of much use in the proof of the next theorem.

Lemma 4 ([48]). *Assume that $V(t)$ is continuous and non-negative and $p_1(t)$ and $p_2(t)$ are both integrable. Then, if additionally for $\alpha \in (0,1)$ and $t \geq t_0$, $V'(t) \leq (p_1(t)+p_2(t))V^{\alpha}(t)$, $\int_{t_0}^{+\infty} p_1(s)ds \leq P$, $\int_{t_0}^{t} p_2(s)ds \leq -\lambda(t-t_0)$, such that P and $\lambda > 0$, it is possible to show that*

$V^{1-\alpha}(t) \leq V^{1-\alpha}(t_0) + (1-\alpha)(P-\lambda(t-t_0)), \forall t \in \left[t_0, T = t_0 + \frac{V^{1-\alpha}(0)+(1-\alpha)P}{\lambda(1-\alpha)}\right]$ *as well as $V(t) = 0$ as long as $t \geq T$.*

Lemma 5 ([49]). *If a real-valued function $w(x)$ is defined on $w(x) \in C^1(\Omega)$, then* $\int_{\Omega} \sum_{k=1}^{m} \left(w(x) \frac{\partial^2 w(x)}{\partial x_k^2} \right) dx \leq \sum_{k=1}^{m} \frac{-\pi^2}{h_k^G - h_k^g} \int_{\Omega} w^2(x)dx.$

Lemma 6 ([50]). *Suppose that $a = (a_1, a_2, ..., a_n)^T$ and $a_i > 0$; then, together with $0 < r < q$, one has $\|a\|_q \leq \|a\|_r \leq n^{\frac{1}{r}-\frac{1}{q}}\|a\|_q$, in which $\|a\|_q = \left(\sum_{k=1}^{n} a_k^q\right)^{\frac{1}{q}}$, while $\|a\|_r = \left(\sum_{k=1}^{n} a_k^r\right)^{\frac{1}{r}}$.*

Throughout the rest of this paper, the notation of $\|e_{ij}(t,x)\|_k = \left(\int_{\Omega} \sum_{(i,j)} e_{ij}^2(t,x)dx\right)^{\frac{1}{k}}$ will be used. Our aim is then to prove the following theorem.

Theorem 3. *If Lemmas 4–6 are all valid with $\int_{t_0}^{+\infty} \rho^+(s)ds \leq P$, $\int_{t_0}^{t} \rho^-(s)ds \leq -\lambda(t-t_0)$, and the controller is defined as $r_{ij}(x,t) = \frac{\rho(t)}{2}\|e_{ij}(t,x)\|_2^{\alpha-1}e_{ij}(t,x) - ce_{ij}(t,x) - sgn(e_{ij}(t,x))$, where $\rho(t) = \rho^+(t) + \rho^-(t)$, that is, the sum of the right and left limits at some point t, then there is a finite-time synchronization between* (4.1) *and* (4.2) *at the time $T = \frac{2\left(\sum_{(i,j)} \int_{\Omega} e_{ij}^2(0,x)dx\right)^{\frac{1-\alpha}{2}} + P(1-\alpha)}{\lambda(1-\alpha)}$.*

Proof. At first, note that

$$Z_{ij}(y(x,t),t)y_{ij}(t,x) - Z_{ij}(\chi(t,x),t)\chi_{ij}(t,x) = \Delta Z(\chi) \leq \left(\bar{C}_{ij}(t) + \bar{E}_{ij}(t) + \bar{D}_{ij}(t)\right) \times [M + L^f|\chi_{ij}(x,t)|],$$

the proof of which is very similar to (2.4). Then construct the following Lyapunov function:

$$V(t) = \sum_{(i,j)} \int_{\Omega} e_{ij}^2(t,x)dx \implies V'(t) = 2\sum_{(i,j)} \int_{\Omega} e_{ij}(t,x)\left[e_{ij}(t,x)\right]_t dx.$$

Thus,

$$V'(t) \leq 2\sum_{(i,j)} \int_{\Omega} r_{ij}(t,x)e_{ij}(t,x)dx + 2\sum_{(i,j)} \int_{\Omega} \left(e_{ij}(t,x)\right)_{xx} e_{ij}(t,x)b_{ij}(t)dx$$

$$- 2\Delta Z(\chi) \int_{\Omega} e_{ij}^2(t,x)dx \tag{4.4}$$

By Lemma 5, the expression is transformed into

$$\begin{aligned}(4.4) \leq & 2\sum_{(i,j)} \int_{\Omega} \left(e_{ij}^2(t,x) \left(\frac{\rho(t)}{2} \|e_{ij}(t,x)\|_2^{\alpha-1} - c \right) - |e_{ij}(t,x)| \right) dx \\ & - 2\left(\sum_{(i,j)} \frac{\pi^2}{h_{ij}^G - h_{ij}^g} + \Delta Z(\chi) \right) \sum_{(i,j)} \int_{\Omega} e_{ij}^2(t,x)dx. \end{aligned} \tag{4.5}$$

Next, exploiting Lemma 6 yields the inequality below:

$$\begin{aligned}(4.5) \leq & \rho(t) \left(\sum_{(i,j)} \int_{\Omega} e_{ij}^2(t,x)dx \right)^{\alpha-1} - 2\sum_{(i,j)} \int_{\Omega} e_{ij}^2(t,x) \left(\sum_{(i,j)} \frac{\pi^2}{h_{ij}^G - h_{ij}^g} + c + \Delta Z(\chi) \right) dx \\ \leq & \rho(t) \left(\sum_{(i,j)} \int_{\Omega} e_{ij}^2(t,x)dx \right)^{\alpha-1} \\ & - 2\sum_{(i,j)} \left(\sum_{(i,j)} \frac{\pi^2}{h_{ij}^G - h_{ij}^g} + c + M\left(\bar{C}_{ij}(t) + \bar{E}_{ij}(t) + \bar{D}_{ij}(t) \right) \right) \int_{\Omega} e_{ij}^2(t,x)dx \\ & - 2L^f \sum_{(i,j)} \int_{\Omega} e_{ij}^2(t,x)\chi_{ij}(x,t)dx \leq \rho(t) \left(\sum_{(i,j)} \int_{\Omega} e_{ij}^2(t,x)dx \right)^{\frac{\alpha+1}{2}} = \left(\rho^+(t) + \rho^-(t) \right) V^{\frac{\alpha+1}{2}}(t). \end{aligned}$$

Hence, by Lemma 4, the time by which both systems should synchronize can consequently be expressed as $T = \frac{2V^{\frac{1-\alpha}{2}}(0) + P(1-\alpha)}{\lambda(1-\alpha)}$.

5. Numerical examples

Finally, we illustrate the results obtained in the previous sections.

5.1. Example 1

Consider (2.1) with $r = z = 1, n = 2, f_{ij}(x) = \frac{1}{2}(|x+1| - |x-1|) \implies M = L^f = 1$, and the functions $a_{ij}(t)$, $C_{ij}(t)$, $L_{ij}(t)$, $B_{ij}(t)$, $U_{ij}(t)$, $D_{ij}(t)$, $E_{ij}(t)$, $T_{ij}(t)$, and $H_{ij}(t)$ given by

$$\begin{bmatrix} a_{11}(t) & a_{12}(t) \end{bmatrix} = \begin{bmatrix} \sin(5t) + 50 & \sin(3t) + 40 \end{bmatrix}$$

$$\begin{bmatrix} C_{11}(t) & C_{12}(t) \end{bmatrix} = \begin{bmatrix} \frac{\cos(4\pi t)}{100} + 0.02 & \frac{\sin(2\pi t)}{100} + 0.025 \end{bmatrix}$$

$$\begin{bmatrix} E_{11}(t) & E_{12}(t) \end{bmatrix} = \begin{bmatrix} \frac{\pi}{90}\sin(2\pi t) + 0.1 & \frac{\pi}{120}\cos(2\pi t) + 0.2 \end{bmatrix}$$

$$\begin{bmatrix} D_{11}(t) & D_{12}(t) \end{bmatrix} = \begin{bmatrix} \frac{\cos(\frac{\pi t}{2})}{500} + 0.01 & \frac{\sin(\frac{\pi t}{2})}{400} + 0.03 \end{bmatrix}$$

$$\begin{bmatrix} H_{11}(t) & H_{12}(t) \end{bmatrix} = \begin{bmatrix} \frac{\cos(t)+1}{2000} & \frac{\cos(t)}{3000} + 0.007 \end{bmatrix}$$

$$\begin{bmatrix} T_{11}(t) & T_{12}(t) \end{bmatrix} = \begin{bmatrix} 0.7\cos(t) + 1.6 & 0.9\sin(t) + 4 \end{bmatrix}$$

$$\begin{bmatrix} B_{11}(t) & B_{12}(t) \end{bmatrix} = \begin{bmatrix} 0.1\sin(\frac{\pi t}{30}) + e & 0.2\sin(\frac{\pi t}{10}) + \frac{\pi e}{6} \end{bmatrix}$$

$$\begin{bmatrix} U_{11}(t) & U_{12}(t) \end{bmatrix} = \begin{bmatrix} \frac{\cos(\pi t)}{1000} + \frac{1}{900} & \frac{\sin(\pi t)}{1000} + \frac{1}{800} \end{bmatrix}$$

$$\begin{bmatrix} L_{11}(t) & L_{12}(t) \end{bmatrix} = \begin{bmatrix} 0.012\sin(t) & 0.01\cos(t) \end{bmatrix}$$

$$\begin{bmatrix} \tau_{11}(t) & \tau_{12}(t) \end{bmatrix} = \begin{bmatrix} 0.015\cos(t) & 0.017\cos(t) \end{bmatrix}$$

$$\begin{bmatrix} x_{11}(0) & x_{12}(0) \end{bmatrix} = \begin{bmatrix} 0.1 & 0.1 \end{bmatrix} \begin{bmatrix} y_{11}(0) & y_{12}(0) \end{bmatrix} = \begin{bmatrix} 0.6 & 0.105 \end{bmatrix}$$

Clearly, (A3) holds as σ is chosen to be 1, $d = H = m = 1 > \frac{1}{2(\underline{a}-1.94)} \approx 0.014$, and

$$\sup\left(L_{ij}(t) + U_{ij}(t) \sum_{C_{kl}\in N_r(i,j)} \left(B_{ij}^{kl}(t) + T_{ij}^{kl}(t) + H_{ij}^{kl}(t) \right) \right) \approx 0.026,$$
$$\sigma\left(1 - M \times \times \sup\left(\sum_{C_{kl}\in N_r(i,j)} C_{ij}^{kl}(t) + D_{ij}^{kl}(t) + E_{ij}^{kl}(t) \right) \right) \approx 0.32,$$

so it is obvious that $\upsilon < \kappa$ as desired. It is not hard to conclude that then synchronization is going to take place before $t^* = \frac{2g\left(g+\sqrt{g^2+d(M(0)+md)}\right)+M(0)d}{d^2}$,; thus, applying $g = 0.5, M(0) = e_{11}^2(0) + e_{12}^2(0)$ brings us to the resultant time of about 2.35. In the presence of inertia, let the next controller's coefficients be exactly the same as above while adding the following:

$$\begin{bmatrix} b_{11}(t) & b_{12}(t) \end{bmatrix} = \begin{bmatrix} \frac{\sin(t/5)}{3} + 5 & \sin(\sqrt{3}t) + 6 \end{bmatrix}$$

$$\begin{bmatrix} x_{11}(0) & x_{12}(0) \end{bmatrix} = \begin{bmatrix} 0.5 & 0.8 \end{bmatrix} \begin{bmatrix} u_{11}(0) & u_{12}(0) \end{bmatrix} = \begin{bmatrix} 0.1 & 0.7 \end{bmatrix}$$

$$\begin{bmatrix} y_{11}(0) & y_{12}(0) \end{bmatrix} = \begin{bmatrix} 0.6 & 0.8 \end{bmatrix} \begin{bmatrix} v_{11}(0) & v_{12}(0) \end{bmatrix} = \begin{bmatrix} 0.3 & 0.2 \end{bmatrix}$$

In this way, $3.37 < b_{ij}(t) < \underline{a} - J + 0.63 \approx 38.9, \underline{a} > 1 + 2(\bar{C} + \bar{D} + \bar{E}) \approx 1.94$, so synchronization will occur by $t_1 = \max\{\frac{K(0)}{l}, e - s\} = \max\{0.1 + 0.4 + 0.3 + 0.6, e - 0.1\} \approx 2.62$.

As for the last model, the functions remain identical to the cases earlier discussed; its initial conditions are $e_1(0, x) = \sinh(x)$ and $e_2(0, x) = x^2$; for the controller the variables are $\alpha = 0.5, c = 1, \rho(t) = \frac{1}{t^2+3} - t|\cos(t)| \implies P \approx 1.6$ and $\lambda \leq 1$. As such, we can expect solutions to synchronize by the following time:

$$T = \frac{2V^{0.5(1-\alpha)}(0) + P(1-\alpha)}{\lambda(1-\alpha)} \approx 1.64.$$

5.2. Example 2

Now let us expand the previous example by taking (2.1) with $f_{ij}(x) = \tanh(x) \implies M = L^f = 1$, and the rest of the functions are defined as follows:

$$\begin{bmatrix} a_{11}(t) & a_{12}(t) & a_{13}(t) \\ a_{21}(t) & a_{22}(t) & a_{23}(t) \end{bmatrix} = \begin{bmatrix} \sin(t)+3 & \cos(t)+4 & \sin(t)+5 \\ \cos(t)+6 & \sin(t)+7 & \cos(t)+8 \end{bmatrix}$$

$$\begin{bmatrix} C_{11}(t) & C_{12}(t) & C_{13}(t) \\ C_{21}(t) & C_{22}(t) & C_{23}(t) \end{bmatrix} = \begin{bmatrix} 0.01\cos(t) & 0.02\sin(t) & 0.05\sin(t) \\ 0.03\cos(t) & 0.04\sin(t) & 0.025\cos(t) \end{bmatrix}$$

$$\begin{bmatrix} E_{11}(t) & E_{12}(t) & E_{13}(t) \\ E_{21}(t) & E_{22}(t) & E_{23}(t) \end{bmatrix} = \begin{bmatrix} \frac{\cos(0.2t)}{\pi^3} & \frac{\sin(0.3t)}{\pi^4} & \frac{\sin(0.25t)}{\pi^5} \\ \frac{\cos(0.1t)}{\pi^2 e} + 0.01 & \frac{\sin(0.2t)}{\pi^3} & \frac{\cos(0.3t)}{\pi^4} \end{bmatrix}$$

$$\begin{bmatrix} D_{11}(t) & D_{12}(t) & D_{13}(t) \\ D_{21}(t) & D_{22}(t) & D_{23}(t) \end{bmatrix} = \begin{bmatrix} \frac{\cos(t^2)}{600} - \frac{1}{400} & \frac{\sin(t^2)}{700} & \frac{\cos(t)}{650} \\ \frac{\sin(t)}{750} & \frac{\cos(t^2)}{700} & \frac{\sin(t)}{650} \end{bmatrix}$$

$$\begin{bmatrix} H_{11}(t) & H_{12}(t) & H_{13}(t) \\ H_{21}(t) & H_{22}(t) & H_{23}(t) \end{bmatrix} = \begin{bmatrix} \frac{\cos(t)+0.5}{2500} & \frac{\cos(t)}{3000} + 0.007 & \frac{\cos(t^2)}{1500} \\ \frac{\sin(t^2)}{2000} & \frac{\cos(t^2)}{2000} & \frac{\sin(t^2)}{1500} \end{bmatrix}$$

$$\begin{bmatrix} T_{11}(t) & T_{12}(t) & T_{13}(t) \\ T_{21}(t) & T_{22}(t) & T_{23}(t) \end{bmatrix} = \begin{bmatrix} 0.6\cos(t)+1.5 & 0.8\sin(t)+3 & 0.5\sin(t) \\ 1-0.3\cos(t) & 0.45\cos(t) & 0.4\sin(t) \end{bmatrix}$$

$$\begin{bmatrix} B_{11}(t) & B_{12}(t) & B_{13}(t) \\ B_{21}(t) & B_{22}(t) & B_{23}(t) \end{bmatrix} = \begin{bmatrix} \frac{\sin(et)}{10} & \frac{\cos(et)}{5} & \sin(et) \\ \cos(et) & \frac{\sin(et)}{20} & \frac{\cos(et)}{20} \end{bmatrix}$$

$$\begin{bmatrix} U_{11}(t) & U_{12}(t) & U_{13}(t) \\ U_{21}(t) & U_{22}(t) & U_{23}(t) \end{bmatrix} = \begin{bmatrix} \sin(\frac{t}{2}) * 10^{-3} & \frac{1}{2}\cos(\frac{t}{2}) * 10^{-3} & \sin(\frac{t-1}{2}) * 10^{-3} \\ \frac{1}{2}\cos(\frac{t-1}{2}) * 10^{-3} & \sin(\frac{t}{2}) * 10^{-4} & \cos(\frac{t}{2}) * 10^{-4} \end{bmatrix}$$

$$\begin{bmatrix} L_{11}(t) & L_{12}(t) & L_{13}(t) \\ L_{21}(t) & L_{22}(t) & L_{23}(t) \end{bmatrix} = \begin{bmatrix} \frac{\sin(t\pi)}{110} & \frac{\cos(t\pi)}{120} & \frac{\sin(t(\pi-1))}{90} \\ \frac{\cos(t(\pi-1))}{95} & \frac{\sin(t\pi)}{105} & \frac{\cos(t\pi)}{115} \end{bmatrix}$$

$$\begin{bmatrix} \tau_{11}(t) & \tau_{12}(t) & \tau_{13}(t) \\ \tau_{21}(t) & \tau_{22}(t) & \tau_{23}(t) \end{bmatrix} = \begin{bmatrix} 0.015\cos(t) & 0.017\cos(t) & 0.015\sin(t) \\ 0.017\sin(t) & 0.016\sin(t) & 0.016\cos(t) \end{bmatrix}$$

$$\begin{bmatrix} x_{11}(0) & x_{12}(0) & x_{13}(0) \\ x_{21}(0) & x_{22}(0) & x_{23}(0) \end{bmatrix} = \begin{bmatrix} -0.15 & 0.65 & 0.3 \\ 0.75 & 0.35 & 0.4 \end{bmatrix} \begin{bmatrix} y_{11}(0) & y_{12}(0) & y_{13}(0) \\ y_{21}(0) & y_{22}(0) & y_{23}(0) \end{bmatrix} = \begin{bmatrix} 0.1 & 0.7 & 0.2 \\ 0.7 & -0.5 & 0.15 \end{bmatrix}$$

(A3) again takes place because when σ equals to 0.5, $d = H = m = 2 > \frac{1}{2(\underline{a}-1-J)} \approx \frac{2}{3}$ and

$$\frac{1}{95} + 10^{-3}\left(2 + 0.4 + 0.5 + 1.3 + 3.8 + 2.1 + 0.4 + 0.45 + \frac{1.5}{2500} + \frac{7}{1000} + \frac{1}{3000} + \frac{1}{1000} + \frac{1}{750}\right)$$

≈ 0.022 being less than

$$0.5\Bigg(1 - 0.04 - 0.05 - 0.03 - 0.01 - 0.02 - 0.025 - \frac{1}{325} - \frac{1}{750} - \frac{1}{600} - \frac{1}{350} - \frac{1}{400} - \frac{1}{\pi^2}\times$$
$$\left(\frac{1}{\pi} + \frac{2}{\pi^2} + \frac{2}{\pi^3} + \frac{1}{e}\right)\Bigg) \approx 0.72.$$

We can then infer that synchronization happens before $t^* = \frac{2\left(1+\sqrt{1+2(1.69+4)}\right)+2*1.69}{4} \approx 3.1$.

For the inertial model (3.1) we also consider the modified parameters:

$$\begin{bmatrix} b_{11}(t) & b_{12}(t) & b_{13}(t) \\ b_{21}(t) & b_{22}(t) & b_{23}(t) \end{bmatrix} = \begin{bmatrix} \frac{\sin(2t)}{3} + 4 & 4 + \frac{\cos(3t)}{5} & \frac{\sin(\frac{\pi t}{2})}{6} + 4 \\ 4 + \frac{\sin(2et)}{4} & 4 + 0.5\sin(t) & 4 + 0.55\cos(0.5t) \end{bmatrix}$$

$$\begin{bmatrix} a_{11}(t) & a_{12}(t) & a_{13}(t) \\ a_{21}(t) & a_{22}(t) & a_{23}(t) \end{bmatrix} = \begin{bmatrix} 3\sin(t) + 10 & 4\cos(t) + 5 & 2\sin(t) + 8 \\ 4\cos(t) + 9 & 2\cos(t) + 9.5 & 3.5\sin(t) + 8.5 \end{bmatrix}$$

$$\begin{bmatrix} x_{11}(0) & x_{12}(0) & x_{13}(0) \\ x_{21}(0) & x_{22}(0) & x_{23}(0) \end{bmatrix} = \begin{bmatrix} -0.15 & 0.65 & 0.2 \\ 0.75 & 0.35 & 0.25 \end{bmatrix} \begin{bmatrix} u_{11}(0) & u_{12}(0) & u_{13}(0) \\ u_{21}(0) & u_{22}(0) & u_{23}(0) \end{bmatrix} = \begin{bmatrix} 0.1 & 0.7 \\ 0.7 & -0.5 \end{bmatrix}$$

$$\begin{bmatrix} y_{11}(0) & y_{12}(0) & y_{13}(0) \\ y_{21}(0) & y_{22}(0) & y_{23}(0) \end{bmatrix} = \begin{bmatrix} 0.0017 & 0.0043 & 0.024 \\ 0.0032 & 0.0001 & 0.0011 \end{bmatrix} \begin{bmatrix} v_{11}(0) & v_{12}(0) & v_{13}(0) \\ v_{21}(0) & v_{22}(0) & v_{23}(0) \end{bmatrix} = \begin{bmatrix} 0.003 & 0.002 & 0.001 \\ 0.0007 & 0 & 0.0018 \end{bmatrix}$$

As a result, $3.37 < b_{ij}(t) < 4.38, \underline{a} > 3$; consequently, the solutions are expected to be synchronized by the time $t_1 = \max\{0.1 + 0.4 + 0.3 + 0.6, e - 2\} \approx 2.62$.

In the diffusion model, all of the functions stay the same, but its initial conditions are defined to be $e_1(0, x) = \sinh(x)$ and $e_2(0, x) = x$. Besides that, $\alpha = 0.4, c = 1, \rho(t) = \frac{1}{t^2+3} - t|\cos(t)| \implies P \approx 1.6$ and $\lambda \leq 1$;therefore, we can expect solutions to synchronize completely at $T \approx 1.32$.

Thus, as a consequence, we can see how some random pair of the matching solutions behave in time with respect to each other in the presence and absence of the proposed designed controller.

6. Discussion

Considering now the obtained graphs, Figures 1(a),(b) and 4(a),(b) demonstrate how the system behaves in the absence of the designed controllers and we observe that there are no visible signs of the synchronization's occurrence up until $t = 1$. On the other hand, once we append the controller to the provided master system, it becomes clear that the curves have already been synchronized by at least $t = 0.14$, as seen in Figures 1(c),(d) and 4(c),(d), so its influence on the neural network is undeniable. This result is also consistent with the theoretical maximal value of 2.35 or later by which we should have seen synchronized curves. In the inertial case (3.1), the situation is more similar to that shown in Figures 2(a),(b) and 5(a),(b) than Figures 2(c),(d) and 5(c),(d). Having the same initial conditions, there were not any indications of potential convergence after $t = 1$. Despite that, after the introduction of the functions $p_{ij}(t)$ and $q_{ij}(t)$, synchronization is clearly completed by $t_{exper} < t_{theor}$, as defined in Theorem 2. Similar to other problems, this is the case because its conditions have been entirely satisfied with the range of functions $b_{ij}(t)$ fixed on the interval (3,5), as well as the sigmoid activation functions. In the end, the diffusion case behaves identically by either diverging completely or at least not synchronizing in Figures 3(a),(b) and 6(a),(b), where after the time $t = 1$ is passed, the solutions begin to actually synchronize rapidly up to $t = 0.006$ and $t = 0.3$, corresponding to Figures 3(c),(d) and 6(c),(d), which can be also represented in three dimensions, as seen in Figures 3(e),(f) and 6(e),(f), respectively. These experimental values of time gained by means of employing the solver of a system of parabolic and elliptic PDEs with one spatial variable x and time t with the time step of 0.0001 supports the theoretical investigation of the latest time at which synchronization completes, i.e., about 1.64. The latter case is displayed in three dimensions including the space variable, where we are looking at the convergence speed of many error curves from the angle from above. Overall, under specified

parameters satisfying the global condition of the activation function being Lipschitz continuous and bounded most of the solutions from drive and response sets are synchronized in finite time and much earlier than the derived settling time.

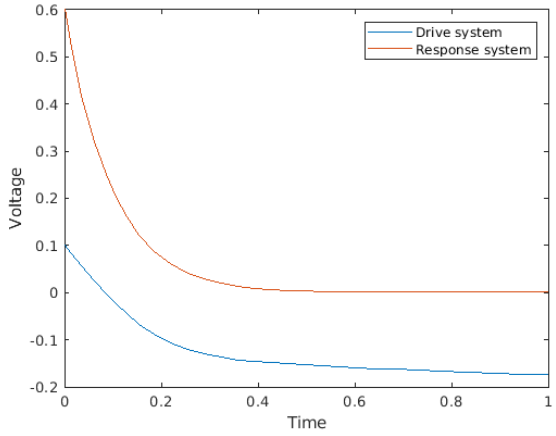

(a) Curves for the drive $x_{11}(t)$ and response $y_{11}(t)$ systems without the controller applied. As can be seen, synchronization between (2.2) and (2.3) is not completed by $t = 1$.

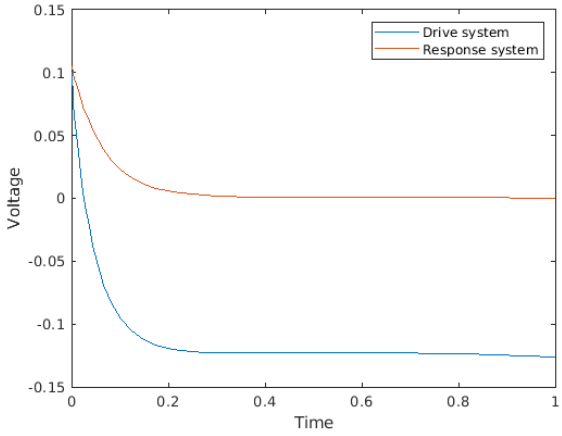

(b) Curves for the drive $x_{12}(t)$ and response $y_{12}(t)$ systems without the controller applied. As can be seen, synchronization between (2.2) and (2.3) is not completed by $t = 1$.

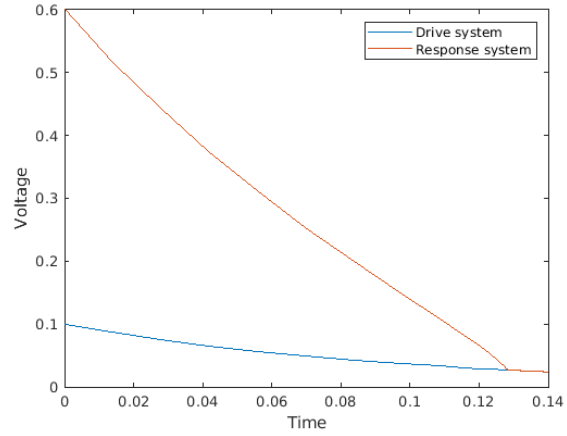

(c) Curves for the drive $x_{11}(t)$ and response $y_{11}(t)$ systems with the controller $p_{11}(t)$ present. From the graph, we can see that (2.2) and (2.3) are synchronized by $t = 0.14$.

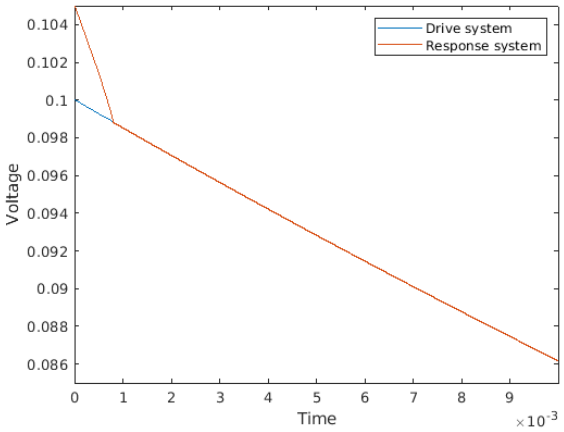

(d) Curves for the drive $x_{12}(t)$ and response $y_{12}(t)$ systems with the controller $p_{12}(t)$ present. From the graph, we can see that (2.2) and (2.3) are synchronized by $t = 0.009$.

Figure 1. Regular FSICNN (2.1).

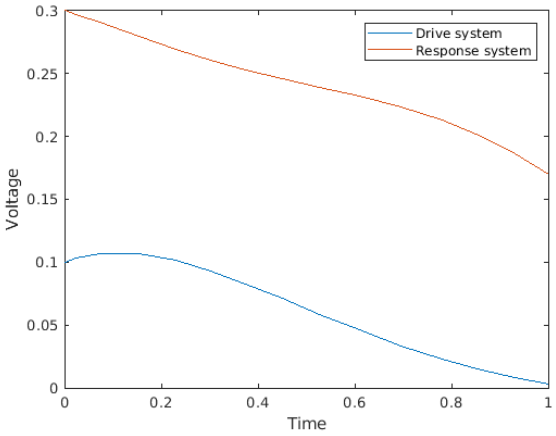

(a) Curves for the drive $v_{11}(t)$ and response $y_{11}(t)$ systems without the controller applied. As can be seen, synchronization between (3.3) and (3.2) is not completed by $t = 1$.

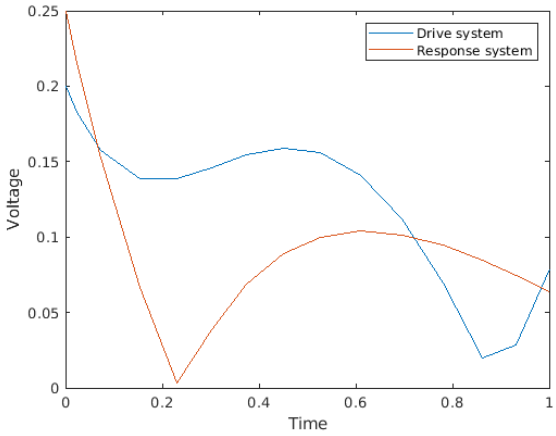

(b) Curves for the drive $v_{12}(t)$ and response $y_{12}(t)$ systems without the controller applied. As can be seen, synchronization between (3.3) and (3.2) is not completed by $t = 1$.

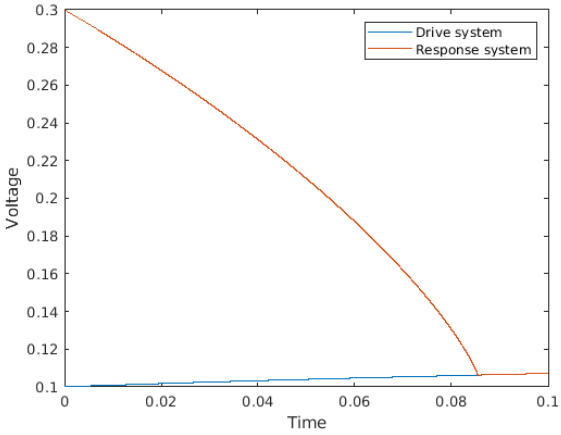

(c) Curves for the drive $v_{11}(t)$ and response $y_{11}(t)$ systems with the controller $q_{11}(t)$ present. From the graph, we can see that (3.3) and (3.2) are synchronized by $t = 0.5$.

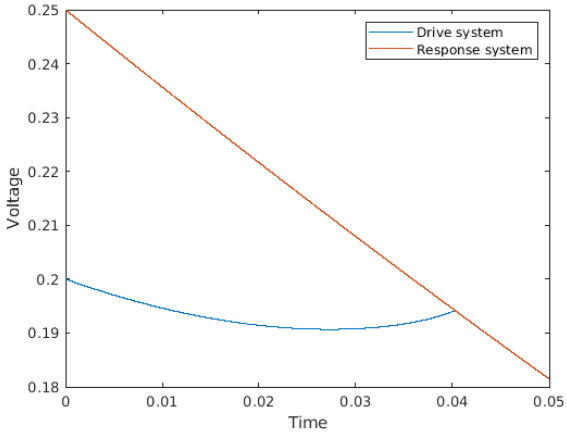

(d) Curves for the drive $v_{12}(t)$ and response $y_{12}(t)$ systems with the controller $q_{12}(t)$ present. From the graph, we can see that (3.3) and (3.2) are synchronized by $t = 0.5$.

Figure 2. FSICNN with the inertial term (3.1).

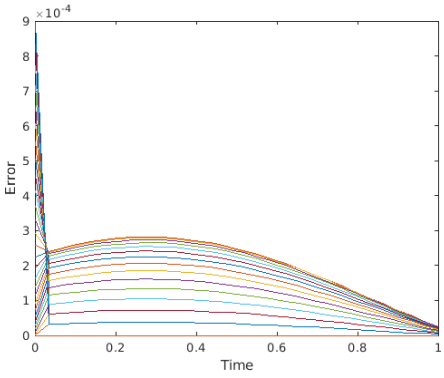

(a) Error curves $e_{11}(t,x)$ for (4.3) without any controller applied. As can be seen, synchronization between (4.1) and (4.2) has not begun by $t = 1$.

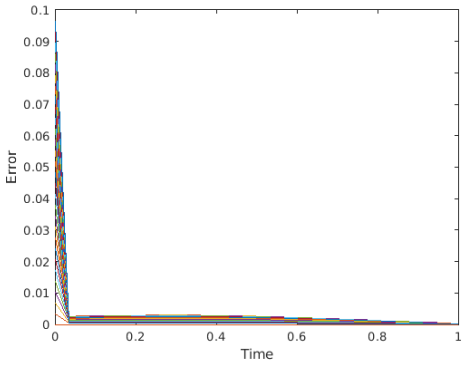

(b) Error curves for $e_{12}(t,x)$ (4.3) without any controller applied. As can be seen, synchronization between (4.1) and (4.2) has not begun by $t = 1$.

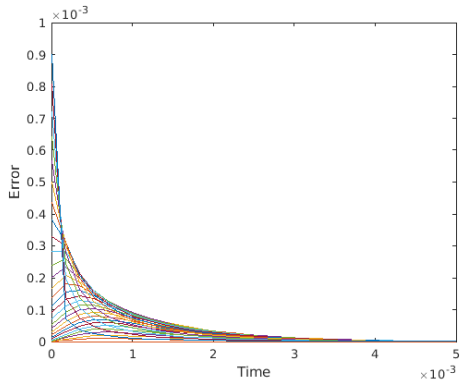

(c) Error curves for $e_{11}(t,x)$ (4.3) with the controller $r_{11}(t)$ present. From the graph, we can see that (4.1) and (4.2) start to synchronize at $t = 0.005$.

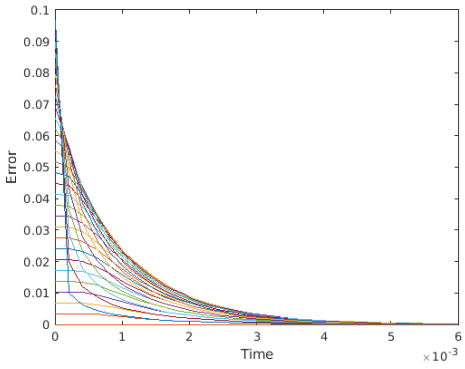

(d) Error curves for $e_{12}(t,x)$ (4.3) with the controller $r_{12}(t)$ present. From the graph, we can see that (4.1) and (4.2) start to synchronize at $t = 0.006$.

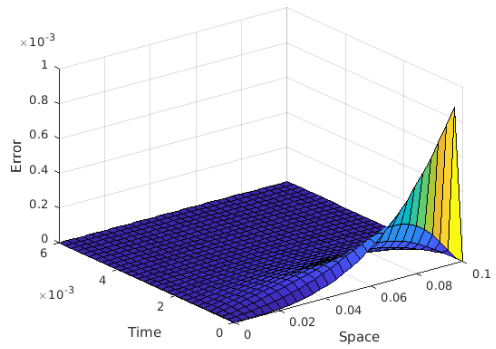

(e) 3D plot corresponding to the case (c) and showing how error reaches zero in space and time.

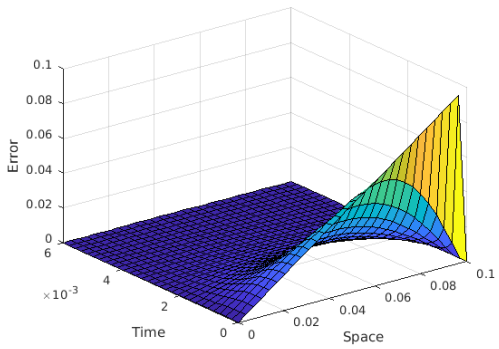

(f) 3D plot corresponding to the case (d) and showing how error reaches zero in space and time.

Figure 3. FSICNN with the diffusion term.

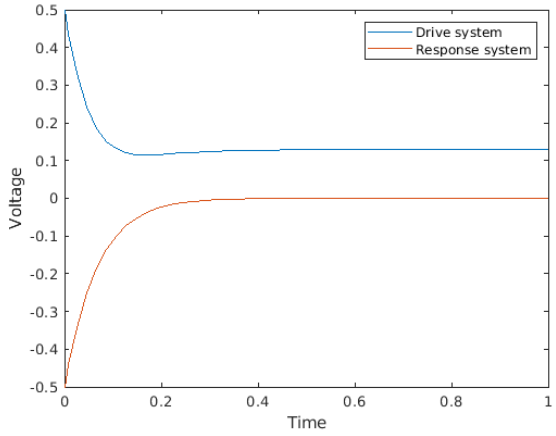

(a) Curves for the drive $x_{21}(t)$ and response $y_{21}(t)$ systems without the controller applied. As can be seen, synchronization between (2.2) and (2.3) is not completed by $t = 1$.

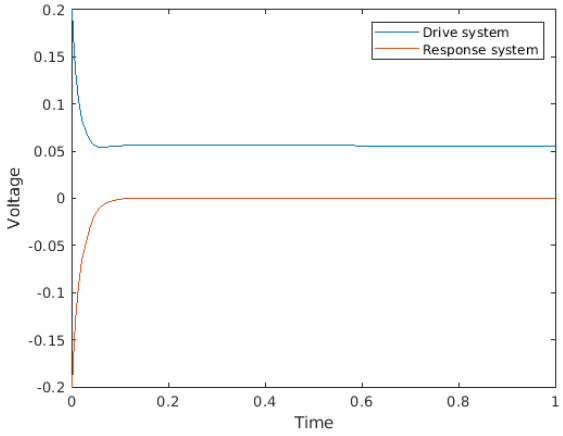

(b) Curves for the drive $x_{22}(t)$ and response $y_{22}(t)$ systems without the controller applied. As can be seen, synchronization between (2.2) and (2.3) is not completed by $t = 1$.

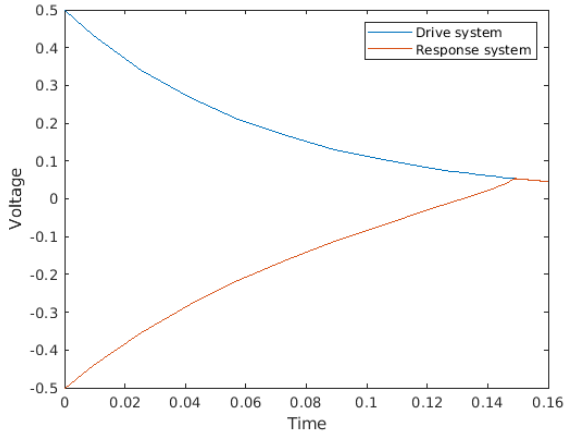

(c) Curves for the drive $x_{21}(t)$ and response $y_{21}(t)$ systems with the controller $p_{11}(t)$ present. From the graph, we can see that (2.2) and (2.3) are synchronized by $t = 0.16$.

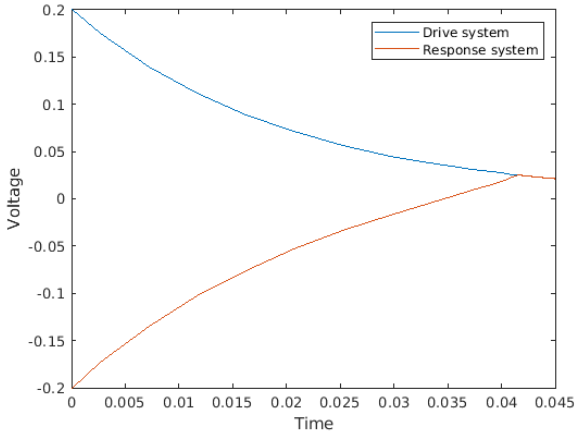

(d) Curves for the drive $x_{22}(t)$ and response $y_{22}(t)$ systems with the controller $p_{12}(t)$ present. From the graph, we can see that (2.2) and (2.3) are synchronized by $t = 0.045$.

Figure 4. Regular FSICNN (2.1).

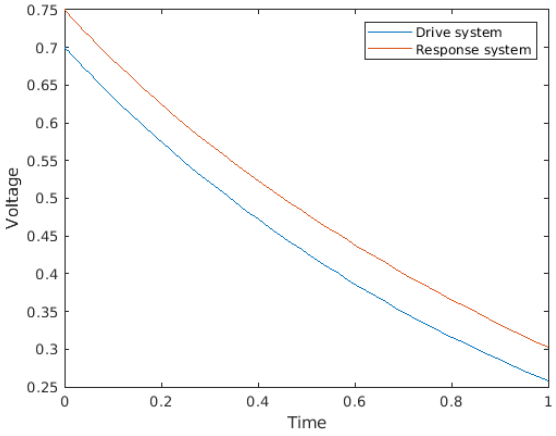

(a) Curves for the drive $u_{21}(t)$ and response $x_{21}(t)$ systems without the controller applied. As can be seen, synchronization between (3.3) and (3.2) is not completed by $t = 1$.

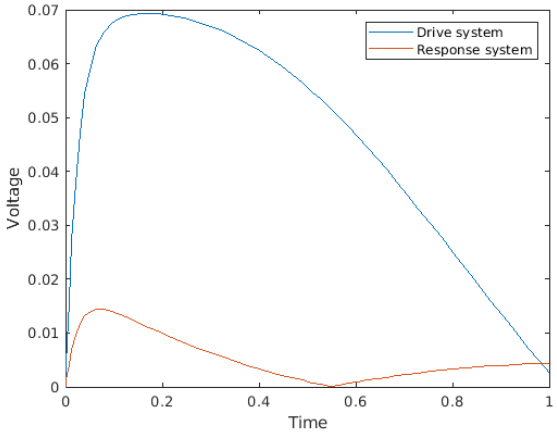

(b) Curves for the drive $v_{22}(t)$ and response $y_{22}(t)$ systems without the controller applied. As can be seen, synchronization between (3.3) and (3.2) is not completed by $t = 1$.

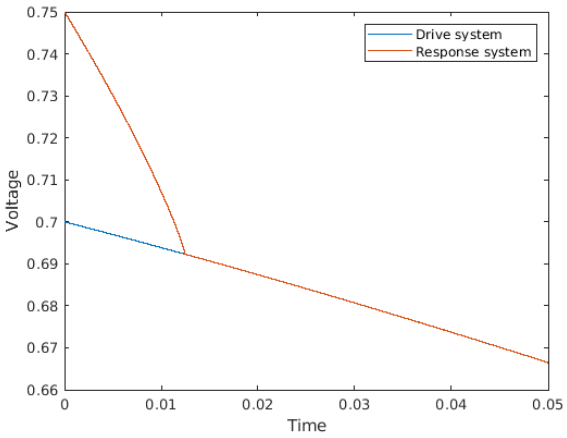

(c) Curves for the drive $u_{21}(t)$ and response $x_{21}(t)$ systems with the controller $p_{21}(t)$ present. From the graph, we can see that (3.3) and (3.2) are synchronized by $t = 0.05$.

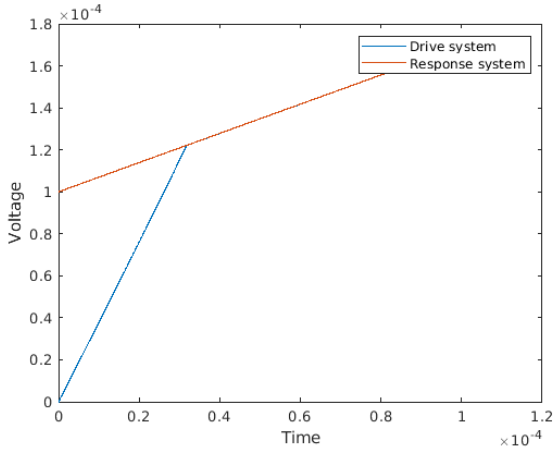

(d) Curves for the drive $v_{22}(t)$ and response $y_{22}(t)$ systems with the controller $q_{22}(t)$ present. From the graph, we can see that (3.3) and (3.2) are synchronized by $t = 10^{-4}$.

Figure 5. FSICNN with the inertial term (3.1).

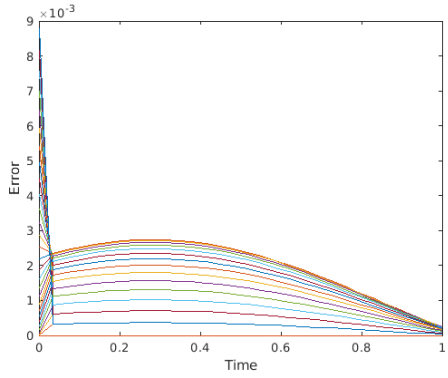

(a) Error curves for $e_{11}(t,x)$ (4.3) without any controller applied. As can be seen, synchronization between (4.1) and (4.2) has not begun by $t = 1$.

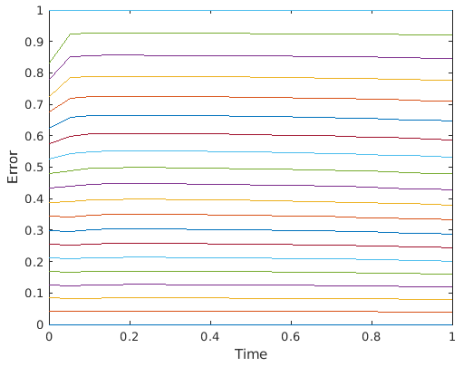

(b) Error curves for $e_{12}(t,x)$ (4.3) without any controller applied. As can be seen, synchronization between (4.1) and (4.2) has not begun by $t = 1$.

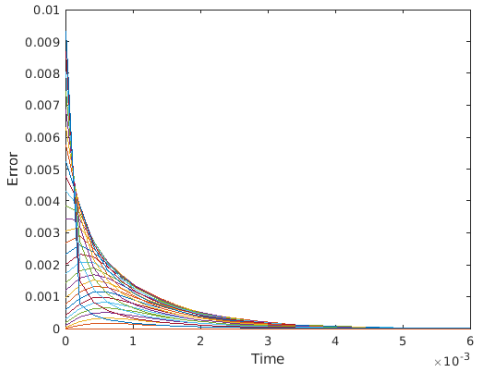

(c) Error curves for $e_{11}(t,x)$ (4.3) with the controller $r_{11}(t)$ present. From the graph, we can see that (4.1) and (4.2) start to synchronize at $t = 0.006$.

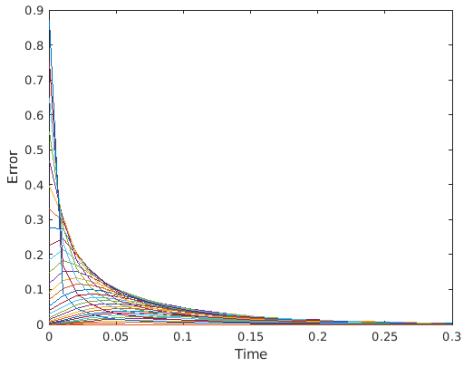

(d) Error curves for $e_{12}(t,x)$ (4.3) with the controller $r_{12}(t)$ present. From the graph, we can see that (4.1) and (4.2) start to synchronize at $t = 0.3$.

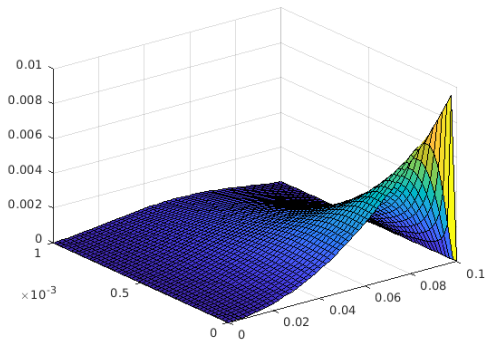

(e) 3D plot corresponding to the case (c) and showing how error reaches zero in space and time.

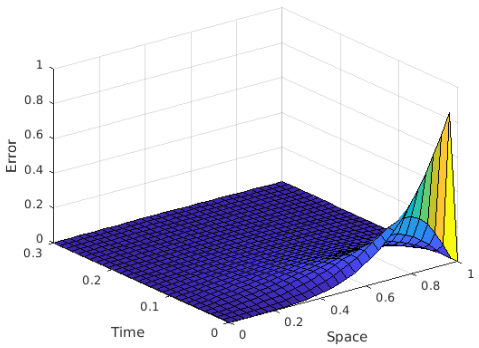

(f) 3D plot corresponding to the case (d) and showing how error reaches zero in space and time.

Figure 6. FSICNN with the diffusion term.

7. Conclusions

In this contribution, we have studied three problems of finite-time synchronization between different sets of master and slave systems. By constructing appropriate Lyapunov functions for each case, we could establish a few sufficient criteria for finite-time synchronization to take place in those drive-response networks, including ordinary FSICNNs and the ones also containing either inertial or diffusion terms. During the analysis, we applied a quite efficient maximum-value technique to prove that the time derivative of the introduced continuous function is non-positive thereby showing the error's convergence to zero. Additionally, three numerical examples and their graphs related to the configuration under consideration have all been shown to support theoretical investigations. Based on all of the facts collected, we were able to infer that under certain controllers after some finite time, the error function is going to diminish, implying that synchronization between two particular equations has been achieved. This study had some limitations in terms of application. One of them is that the resulting synchronization time in those scenarios is not perfect and observation of this time requires much computational power for large systems. In addition, the assumptions of Lipschitz continuity along with boundedness significantly reduce the choice for the activation function. Further, we considered a range of parameters that were not verified by real experiments. Thus, two or more types of mixed uncertainties should also be taken into account in future studies. Moreover, the studies will be improved by reducing the maximal time of expected synchronization through the construction of more elegant Lyapunov functions and controllers, which can result in more relaxed preliminary assumptions along with the possibility of switching to a more powerful fixed-time synchronization between systems. Finally, the corresponding fractional-order system can be examined instead, incorporating singularities to check the optimal order and fractional calculus lemmas, such as the fractional Halanay inequality.

Use of AI tools declaration

The authors declare they have not used Artificial Intelligence (AI) tools in the creation of this article.

Acknowledgements

This research was funded by the Committee of Science of the Ministry of Science and Higher Education of the Republic of Kazakhstan (grant no. AP13068282 "Synchronization and anti-synchronization analysis of discrete-time neural networks with delays").

Conflict of interest

The authors declare that there are no conflicts of interest regarding the publication of this manuscript.

References

1. G. Velmurugan, R. Rakkiyappan, J. D. Cao, Finite-time synchronization of fractional-order memristor-based neural networks with time delays, *Neural Networks*, **73** (2016), 36–46. https://doi.org/10.1016/j.neunet.2015.09.012

2. A. Bouzerdoum, Classification and function approximation using feed-forward shunting inhibitory artificial neural networks, In: *Proceedings Of The IEEE-INNS-ENNS International Joint Conference On Neural Networks. IJCNN 2000. Neural Computing: New Challenges And Perspectives For The New Millennium*, 2000, 613–618. https://doi.org/10.1109/IJCNN.2000.859463

3. F. H. C. Tivive, A. Bouzerdoum, A face detection system using shunting inhibitory convolutional neural networks, In: *2004 IEEE International Joint Conference On Neural Networks*, 2004, 2571–2575. https://doi.org/10.1109/IJCNN.2004.1381049

4. S. Yan, Z. Gu, Ju. H. Park, X. P. Xie, Synchronization of delayed fuzzy neural networks with probabilistic communication delay and its application to image encryption, *IEEE Trans. Fuzzy Syst.*, **31** (2023), 930–940. https://doi.org/10.1109/TFUZZ.2022.3193757

5. H. M. Oliveira, L. V. Melo, Huygens synchronization of two clocks, *Sci. Rep.*, **5** (2015), 11548. https://doi.org/10.1038/srep11548

6. S. Y. Dong, X. Z. Liu, S. M. Zhong, K. B. Shi, H. Zhu, Practical synchronization of neural networks with delayed impulses and external disturbance via hybrid control, *Neural Networks*, **157** (2023), 54–64. https://doi.org/10.1016/j.neunet.2022.09.025

7. C. Xu, X. S. Yang, J. Q. Lu, J. W. Feng, F. E. Alsaadi, T. Hayat, Finite-time synchronization of networks via quantized intermittent pinning control, *IEEE Trans. Cybernetics*, **48** (2018), 3021–3027. https://doi.org/10.1109/TCYB.2017.2749248

8. X. Y. Liu, H. S. Su, M. Z. Q. Chen, A switching approach to designing finite-time synchronization controllers of coupled neural networks, *IEEE Trans. Neur. Net. Lear.*, **27** (2015), 471–482. https://doi.org/10.1109/TNNLS.2015.2448549

9. P. Pucci, J. Serrin, *The maximum principle*, Basel: Birkhäuser, 2007. https://doi.org/10.1007/978-3-7643-8145-5

10. V. Zeidan, C. Nour, H. Saoud, A nonsmooth maximum principle for a controlled nonconvex sweeping process, *J. Differ. Equations*, **269** (2020), 9531–9582. https://doi.org/10.1016/j.jde.2020.06.053

11. Q. Du, L. L. Ju, X. Li, Z. H. Qiao, Maximum principle preserving exponential time differencing schemes for the nonlocal Allen–Cahn equation, *SIAM J. Numer. Anal.*, **57** (2019), 875–898. https://doi.org/10.1137/18M118236X

12. A. Kashkynbayev, M. Koptileuova, A. Issakhanov, J. D. Cao, Almost periodic solutions of fuzzy shunting inhibitory CNNs with delays, *AIMS Mathematics*, **7** (2022), 11813–11828. https://doi.org/10.3934/math.2022659

13. X. G. Tan, C. C. Xiang, J. D. Cao, W. Y. Xu, G. H. Wen, L. Rutkowski, Synchronization of neural networks via periodic self-triggered impulsive control and its application in image encryption, *IEEE Trans. Cybernetics*, **52** (2022), 8246–8257. https://doi.org/10.1109/TCYB.2021.3049858

14. Y. Wang, S. B. Ding, R. X. Li, Master–slave synchronization of neural networks via event-triggered dynamic controller, *Neurocomputing*, **419** (2021), 215–223. https://doi.org/10.1016/j.neucom.2020.08.062

15. F. Liu, C. Liu, H. X. Rao, Y. Xu, T. W. Huang, Reliable impulsive synchronization for fuzzy neural networks with mixed controllers, *Neural Networks*, **143** (2021), 759–766. https://doi.org/10.1016/j.neunet.2021.08.013

16. L. Y. Duan, J. M. Li, Fixed-time synchronization of fuzzy neutral-type BAM memristive inertial neural networks with proportional delays, *Inform. Sciences*, **576** (2021), 522–541. https://doi.org/10.1016/j.ins.2021.06.093

17. M. Abudusaimaiti, A. Abdurahman, H. J. Jiang, C. Hu, Fixed/predefined-time synchronization of fuzzy neural networks with stochastic perturbations, *Chaos Soliton. Fract.*, **154** (2022), 111596. https://doi.org/10.1016/j.chaos.2021.111596

18. X. N. Li, H. Q. Wu, J. D. Cao, A new prescribed-time stability theorem for impulsive piecewise-smooth systems and its application to synchronization in networks, *Appl. Math. Model.*, **115** (2023), 385–397. https://doi.org/10.1016/j.apm.2022.10.051

19. X. N. Li, H. Q. Wu, J. D. Cao, Prescribed-time synchronization in networks of piecewise smooth systems via a nonlinear dynamic event-triggered control strategy, *Math. Comput. Simulat.*, **203** (2023), 647–668. https://doi.org/10.1016/j.matcom.2022.07.010

20. X. Z. Jin, G. H. Yang, Adaptive pinning synchronization of a class of nonlinearly coupled complex networks, *Commun. Nonlinear Sci.*, **18** (2013), 316–326. https://doi.org/10.1016/j.cnsns.2012.07.011

21. Q. Chen, B. Li, W. Yin, X. W. Jiang, X. Y. Chen, Bifurcation, chaos and fixed-time synchronization of memristor cellular neural networks, *Chaos Soliton. Fract.*, **171** (2023), 113440. https://doi.org/10.1016/j.chaos.2023.113440

22. F. F. Du, J.-G. Lu, Adaptive finite-time synchronization of fractional-order delayed fuzzy cellular neural networks, *Fuzzy Set. Syst.*, **466** (2023), 108480. https://doi.org/10.1016/j.fss.2023.02.001

23. X. Z. Jin, J. H. Jiang, J. Chi, X. M. Wu, Adaptive finite-time pinned and regulation synchronization of disturbed complex networks, *Commun. Nonlinear Sci.*, **124** (2023), 107319. https://doi.org/10.1016/j.cnsns.2023.107319

24. J. H. Jiang, X. Z. Jin, J. Chi, X. M. Wu, Distributed adaptive fixed-time synchronization for disturbed complex networks, *Chaos Soliton. Fract.*, **173** (2023), 113612. https://doi.org/10.1016/j.chaos.2023.113612

25. C. J. Cheng, T. L. Liao, C. C. Hwang, Exponential synchronization of a class of chaotic neural networks, *Chaos Soliton. Fract.*, **24** (2005), 197–206. https://doi.org/10.1016/j.chaos.2004.09.022

26. M. H. Protter, H. F. Weinberger, *Maximum principles in differential equations*, New York: Springer, 1984. https://doi.org/10.1007/978-1-4612-5282-5

27. T. Yang, L.-B. Yang, C. W. Wu, L. O. Chua, Fuzzy cellular neural networks: applications, In: *1996 Fourth IEEE International Workshop On Cellular Neural Networks And Their Applications Proceedings (CNNA-96)*, 1996, 225–230. https://doi.org/10.1109/CNNA.1996.566560

28. T. Yang, L. B. Yang, Fuzzy cellular neural network: a new paradigm for image processing, *Int. J. Circ. Theor. Appl.*, **25** (1997), 469–481. https://doi.org/10.1002/(SICI)1097-007X(199711/12)25:6¡469::AID-CTA967¿3.0.CO;2-1

29. P. V. De Campos Souza, Fuzzy neural networks and neuro-fuzzy networks: a review the main techniques and applications used in the literature, *Appl. Soft Comput.*, **92** (2020), 106275. https://doi.org/10.1016/j.asoc.2020.106275

30. A. Kashkynbayev, J. D. Cao, Z. Damiyev, Stability analysis for periodic solutions of fuzzy shunting inhibitory CNNs with delays, *Adv. Differ. Equ.*, **2019** (2019), 384. https://doi.org/10.1186/s13662-019-2321-z

31. S. C. Lee, E. T. Lee, Fuzzy neural networks, *Math. Biosci.*, **23** (1975), 151–177. https://doi.org/10.1016/0025-5564(75)90125-X

32. M. M. Gupta, D. H. Rao, On the principles of fuzzy neural networks, *Fuzzy Set. Syst.*, **61** (1994), 1–18. https://doi.org/10.1016/0165-0114(94)90279-8

33. T. Yang, L.-B. Yang, The global stability of fuzzy cellular neural network, *IEEE Trans. Circuits Syst. I*, **43** (1996), 880–883. https://doi.org/10.1109/81.538999

34. A. Kashkynbayev, A. Issakhanov, M. Otkel, J. Kurths, Finite-time and fixed-time synchronization analysis of shunting inhibitory memristive neural networks with time-varying delays, *Chaos Soliton. Fract.*, **156** (2022), 111866. https://doi.org/10.1016/j.chaos.2022.111866

35. C. Foias, G. R. Sell, R. Temam, Inertial manifolds for nonlinear evolutionary equations, *J. Differ. Equations*, **73** (1988), 309–353. https://doi.org/10.1016/0022-0396(88)90110-6

36. E. S. Titi, On approximate inertial manifolds to the Navier-Stokes equations, *J. Math. Anal. Appl.*, **149** (1990), 540–557. https://doi.org/10.1016/0022-247X(90)90061-J

37. M. S. Jolly, I. G. Kevrekidis, E. S. Titi, Approximate inertial manifolds for the Kuramoto-Sivashinsky equation: analysis and computations, *Physica D*, **44** (1990), 38–60. https://doi.org/10.1016/0167-2789(90)90046-R

38. J. D. Cao, Y. Wan, Matrix measure strategies for stability and synchronization of inertial BAM neural network with time delays, *Neural Networks*, **53** (2014), 165–172. https://doi.org/10.1016/j.neunet.2014.02.003

39. S. Lakshmanan, M. Prakash, C. P. Lim, R. Rakkiyappan, P. Balasubramaniam, S. Nahavandi, Synchronization of an inertial neural network with time-varying delays and its application to secure communication, *IEEE Trans. Neur. Net. Lear.*, **29** (2018), 195–207. https://doi.org/10.1109/TNNLS.2016.2619345

40. X. Y. Li, X. T. Li, C. Hu, Some new results on stability and synchronization for delayed inertial neural networks based on non-reduced order method, *Neural Networks*, **96** (2017), 91–100. https://doi.org/10.1016/j.neunet.2017.09.009

41. W. H. Li, X. B. Gao, R. X. Li, Stability and synchronization control of inertial neural networks with mixed delays, *Appl. Math. Comput.*, **367** (2020), 124779. https://doi.org/10.1016/j.amc.2019.124779

42. Z. Q. Zhang, J. D. Cao, Finite-time synchronization for fuzzy inertial neural networks by maximum value approach, *IEEE Trans. Fuzzy Syst.*, **30** (2022), 1436–1446. https://doi.org/10.1109/TFUZZ.2021.3059953

43. J.-L. Wang, H.-N. Wu, T. W. Huang, S.-Y. Ren, Pinning control strategies for synchronization of linearly coupled neural networks with reaction–diffusion terms, *IEEE Trans. Neur. Net. Lear.*, **27** (2016), 749–761. https://doi.org/10.1109/TNNLS.2015.2423853

44. Y. Y. Cao, Y. T. Cao, Z. Y. Guo, T. W. Huang, S. P. Wen, Global exponential synchronization of delayed memristive neural networks with reaction–diffusion terms, *Neural Networks*, **123** (2020), 70–81. https://doi.org/10.1016/j.neunet.2019.11.008

45. Q. Ma, S. Y. Xu, Y. Zou, G. D. Shi, Synchronization of stochastic chaotic neural networks with reaction-diffusion terms, *Nonlinear Dyn.*, **67** (2012), 2183–2196. https://doi.org/10.1007/s11071-011-0138-8

46. L. Shanmugam, P. Mani, R. Rajan, Y. H. Joo, Adaptive synchronization of reaction–diffusion neural networks and its application to secure communication, *IEEE Trans. Cybernetics*, **50** (2020), 911–922. https://doi.org/10.1109/TCYB.2018.2877410

47. C. Hu, H. J. Jiang, Z. D. Teng, Impulsive control and synchronization for delayed neural networks with reaction–diffusion terms, *IEEE Trans. Neural Network.*, **21** (2010), 67–81. https://doi.org/10.1109/TNN.2009.2034318

48. Z. Y. Wang, J. D. Cao, Z. W. Cai, X. G. Tan, R. S. Chen, Finite-time synchronization of reaction-diffusion neural networks with time-varying parameters and discontinuous activations, *Neurocomputing*, **447** (2021), 272–281. https://doi.org/10.1016/j.neucom.2021.02.065

49. Z. Y. Wang, J. D. Cao, Z. W. Cai, L. Rutkowski, Anti-synchronization in fixed time for discontinuous reaction–diffusion neural networks with time-varying coefficients and time delay, *IEEE Trans. Cybernetics*, **50** (2020), 2758–2769. https://doi.org/10.1109/TCYB.2019.2913200

50. G. H. Hardy, J. E. Littlewood, G. Pólya, *Inequalities*, Cambridge university press, 1952.